Inhibition Mechanism of the Recombinant Rat P2X 2 Receptor in Glial Cells by Suramin and TNP−ATP †

ARTICLE *in* BIOCHEMISTRY · FEBRUARY 2006

Impact Factor: 3.02 · DOI: 10.1021/bi051517w · Source: PubMed

Inhibition Mechanism of the Recombinant Rat $P2X_2$ Receptor in Glial Cells by Suramin and TNP-ATP†

Cleber A. Trujillo,‡ Arthur A. Nery,‡ Antonio Henrique B. Martins,§ Paromita Majumder,‡ Fernando A. Gonzalez,|| and Henning Ulrich*,‡

Departamento de Bioquímica, Instituto de Química, Universidade de São Paulo, São Paulo 05508-900, Brazil, Departamento de Biofísica, Universidade Federal de São Paulo, São Paulo 04023-62, Brazil, and Department of Chemistry, University of Puerto Rico, San Juan, Puerto Rico 00931-3346

Received July 29, 2005; Revised Manuscript Received October 17, 2005

ABSTRACT: P2X receptors play an important role in communication between cells in the nervous system. Therefore, understanding the mechanisms of inhibition of these receptors is important for the development of new tools for drug discovery. Our objective has been to determine the pharmacological activity of the antagonist suramin, the most important antagonist of purinergic receptor function, as well as to demonstrate its noncompetitive inhibition and confirm a competitive mechanism between ATP and TNP-ATP in 1321N1 glial cells stably transfected with the recombinant rat $P2X_2$ receptor. A radioligand binding assay was employed to determine whether suramin, TNP-ATP, and ATP compete for the same binding site on the receptor. TNP-ATP displaced [α-^{32}P]ATP, whereas suramin did not interfere with [α-^{32}P]ATP−receptor binding. To determine the inhibition mechanism relevant for channel opening, currents obtained in fast kinetic whole-cell recording experiments, following stimulation of cells by ATP in the presence of suramin, were compared to those obtained by ATP in the presence of TNP-ATP. Supported by a mathematical model for receptor kinetics [Breitinger, H. G., Geetha, N., and Hess, G. P. (2001) *Biochemistry 40,* 8419−8429], the inhibition factors were plotted as functions of inhibitor or agonist concentrations. Analysis of the data indicated a competitive inhibition mechanism for TNP-ATP and a noncompetitive inhibition for suramin. Taken together, both data support a noncompetitive inhibition mechanism of the rat recombinant $P2X_2$ receptor by suramin, confirm the competitive inhibition by TNP-ATP, and allow the prediction of a model for $P2X_2$ receptor inhibition.

The biological effects of extracellular purine nucleotides acting through P2 receptors have been studied in many cell and tissue types. ATP is now recognized as an important messenger molecule in cell−cell communication in the central nervous system and has been shown to be involved in brain development (*1*−*3*). The P2X receptors are formed from seven distinct gene products encoding different ATP-gated ion channel subunits (*4*). The P2X receptor has a distinctive structural motif, with each subunit containing two hydrophobic transmembrane domains connected by a large intervening hydrophilic extracellular loop (*5*). The protein subunits combine as either homomultimers or heteromultimers to form functional membrane-spanning multimeric receptors (*6*−*9*). The inclusion of multiple subunits into a functional receptor can confer distinct biophysical and pharmacological properties to a particular receptor subtype (*10*, *11*).

According to Ding and Sachs (*12*), the best model with which to describe the channel opening of P2X receptors can be summarized as follows. (I) The channel proceeds through three ATP binding steps before opening. (II) The three ATP binding sites are positively cooperative. (III) There are two open states, which connect to a common ATP-independent closed state. (IV) Activation and deactivation proceed along the same pathway. (V) Channels open only after having bound to three ligand molecules.

The pharmacological investigation of P2X receptors has been hampered by the lack of potent subtype-selective ligands and antagonists. Antagonists, such as suramin, 2′,3′-*O*-(2,4,6-trinitrophenyl)adenosine 5′-triphosphate (TNP-ATP),[1] and their analogues have traditionally been used as P2X receptor antagonists (*13*−*16*). Moreover, these compounds are relatively nonselective and exhibit nanomolar to micromolar binding affinities for P2X receptors (*16*−*18*), and the mechanism of inhibition of the receptor by these compounds is not yet well understood.

Dunn and Blakeley (*19*) were the first to demonstrate that suramin antagonizes purinergic receptor activity. In many

† This work was supported by a research grant from Fundação de Amparo à Pesquisa do Estado de São Paulo (FAPESP), Project 2001/08827-4, Brazil, awarded to H.U.; C.A.T. and P.M. are supported by fellowships by FAPESP. A.A.N. and A.H.M. are supported by fellowships from Conselho Nacional de Desenvolvimento Científico (CNPq) and Coordenação de Aperfeiçoamento de Pessoal de Nível Superior (CAPES), Brazil, respectively. F.A.G. acknowledges support from the National Institutes of Health through Grant GM-08102.

* To whom correspondence should be addressed. E-mail: henning@iq.usp.br. Telephone: +55-11-3091-3810, ext. 223. Fax: +55-11-3815-5579.

‡ Universidade de São Paulo.

§ Universidade Federal de São Paulo.

|| University of Puerto Rico.

[1] Abbreviation: TNP-ATP, 2′,3′-*O*-(2,4,6-trinitrophenyl)adenosine 5′-triphosphate.

10.1021/bi051517w CCC: $33.50
Published on Web 12/13/2005

studies, suramin has been reported to be one of the mainly important, nonselective, and reversible inhibitors of these receptors (*20*−*23*). In most cases, suramin has been described as a competitive inhibitor displacing ATP from the ligand-binding site of the receptor (*24*−*27*). This conclusion is based on the effect of these compounds on dose−effect curves induced by the purinergic receptor agonist α,β-methylene-ATP in the presence of suramin (*24*), competition of suramin with α,β-methylene-ATP for receptor binding as determined by autoradiographic studies of rat brain sections (*25*), and electrophysiological studies with recombinant receptors expressed in oocytes and cells (*26*, *27*). However, results obtained by Wong and collaborators (*28*) from single-channel measurements using rat hippocampus patches indicated that the inhibitory effect of suramin on P2X receptor activity was inconsistent with a simple competitive antagonism model.

The ATP analogue TNP-ATP has been used for labeling ATP-binding sites in a variety of tissues (*29*, *30*). Mockett et al. (*31*) and King et al. (*32*) were among the first to describe antagonist effects of TNP-ATP on P2X receptors. This potent and relatively selective P2X receptor antagonist has recently been used to characterize a variety of native P2X receptors (*33*−*36*).

TNP-ATP is a close structural analogue of ATP, suggesting that it may bind to the extracellular ATP binding pocket of P2X receptors, and may act as a competitive antagonist. This appeared to be the case when nondesensitizing ATP responses on cochlear hair cells were blocked by TNP-ATP in a competitive manner (*31*). Experiments published by Burgard and colleagues (*37*) also indicated a competitive inhibition mechanism. However, Virginio et al. (*38*) described TNP-ATP as a noncompetitive antagonist of rapidly desensitizing recombinant rat $P2X_3$ receptors.

In an attempt to elucidate the inhibition mechanism of suramin and TNP-ATP and to provide a strong basis for further pharmacological analysis of P2X receptors, we have examined the mechanism of inhibition of a recombinant $P2X_2$ receptor by suramin and by TNP-ATP. Our results suggest that suramin behaves as a noncompetitive antagonist, binding to a different site on the receptor compared to ATP, and confirm the competitive action of TNP-ATP.

MATERIALS AND METHODS

Material. Unless otherwise indicated, all reagents were purchased from Sigma and were of the highest available quality. [α-^{32}P]ATP (3.000 Ci/mmol) was from Amersham.

Cell Culture and Maintenance. Human 1321N1 astrocytoma cells expressing recombinant rat $P2X_2$ receptors, as already described for the recombinant $P2Y_2$ receptors (*39*, *40*), were grown in Dulbecco's modified Eagle's medium (DMEM, high glucose, Invitrogen) supplemented with 10% (v/v) fetal bovine serum (Cultilab, Campinas, Brazil) in the presence of 100 IU/mL penicillin, 100 μg/mL streptomycin, and 0.5 mg/mL Geneticin (Sigma) at 37 °C in a water-saturated atmosphere containing 5% CO_2. Cell cultures were subcultured weekly, seeded at 5×10^5 cells/culture flask (175 cm^2), and fed three times during that period by replacing the old medium. For electrophysiology, 2×10^4 cells were plated into 35 mm cell culture dishes and used for experiments within 2−4 days.

Whole-Cell Recording. Recording glass pipets were pulled from borosilicate glass (World Precision Instruments Inc., Berlin, Germany), using a two-stage puller (Sutter P-10, Sutter Instruments, Novato, CA). Pipet tips were fire-polished using a flame polisher (MF-83, Narishige, Tokyo, Japan). The extracellular recording buffer contained 145 mM NaCl, 5.3 mM KCl, 1.8 mM $CaCl_2 \cdot 2H_2O$, 1.2 mM $MgCl_2$, 10 mM glucose, and 10 mM HEPES; the pH was adjusted to 7.4 with NaOH. The intracellular solution contained 140 mM KCl, 10 mM NaCl, 2 mM $MgCl_2$, 1 mM EGTA, and 10 mM HEPES; the pH was adjusted to 7.4 with KOH. An Axopatch 200A amplifier and the pClamp software packet (Molecular Devices Corp., Union City, CA) were used for data collection. The obtained data were analyzed on a personal computer using Microcal Origin (Northampton, MA). All measurements were carried out at pH 7.4 and 21−23 °C at a transmembrane voltage of −60 mV. Data from each cell were normalized to the response measured with 100 μM ATP. All solutions used in the experiments were prepared on the day of the measurement.

The flow method used for rapid ligand application has been described by Krishtal and Pidoplichko (*41*) and Udgaonkar and Hess (*42*). Briefly, a cell in the whole-cell recording configuration (*43*) was placed ca. 100 μm from the porthole (diameter of ca. 100 μm) of a U-tube (Hamilton, Reno, NV) (*41*). The flow rate of solutions emerging from the flow device, containing neurotransmitter with or without inhibitor, was typically 1 cm/s. Measurements were taken in intervals of 5 min, a time sufficient to allow for recovery of desensitized receptors (*44*).

Western Blotting. 1321N1 glial cells were resuspended in PBS (phosphate-buffered saline) with 2 mM EDTA. Cell lyses was started by sonication (3 × 10 pulses at 30%) in the presence of protease inhibitors. The material was centrifuged for 15 min at 3000*g* and 4 °C, and the supernatant was collected. The supernatant was ultracentrifuged for 1.5 h at 100000*g* and 4 °C, and the pellet was resuspended in 50 mM HEPES (pH 7.4).

Forty micrograms of membrane proteins from ultracentrifugation was mixed with SDS−PAGE sample buffer containing 0.05% (v/v) mercaptoethanol, heated for 5 min to 95 °C, separated on 10% SDS−polyacrylamide gels, and electroblotted onto nitrocellulose membranes (Transblot, 0.45 μm, Bio-Rad). The membranes were incubated with a blocking solution containing 3% nonfat milk powder in PBS-T (PBS with 0.05% Tween 20) for 30 min at room temperature, followed by overnight incubation at 4 °C with a 1/250 dilution of goat polyclonal anti-$P2X_2$ antibody (Santa Cruz Biotechnology, Heidelberg, Germany) in the same blocking solution. Following three washes with PBS-T, membranes were incubated for 2 h at room temperature with peroxidase-conjugated secondary anti-goat IgG (1/100) (Santa Cruz Biotechnology). Reactions were developed by using the ECL plus kit (Pierce) according to the instructions provided by the manufacturer.

Radioligand Binding Assay. Radioligand binding methodology was generally adapted from procedures described by Michel et al. (*45*) and modified to enhance specific binding to living cells expressing rat $P2X_2$ receptors. 1321N1 human glioma cells (200 000) expressing the recombinant $P2X_2$ receptor were incubated for 30 min at 25 °C in PBS at pH 7.4 with [α-^{32}P]ATP (200 000 cpm, 130 pM) in the absence or presence of increasing concentrations of the antagonists suramin and TNP-ATP to determine whether

suramin, TNP-ATP, and [α-^{32}P]ATP compete for the same binding site. The percentage of nonspecific binding of [α-^{32}P]-ATP was determined in the presence of 100 μM unlabeled ATP.

Following incubation, the cells were washed three times with PBS, solubilized in the presence of SDS (1%), and transferred to scintillation vials. Receptor-bound [α-^{32}P]ATP was quantified by scintillation counting. Protein concentrations were determined as described by Bradford (*46*).

Data Analysis. The relation between *A*, the measured whole-cell current amplitude, and the concentration of open receptor channels was derived for the acetylcholine receptor (*47*, *48*), and the equation was then adapted to apply to cell-flow measurements (*42*). When the initial ligand concentration is much larger than the number of moles of receptor in the absence of desensitization, this relation is given by (*49*)

$$A = I_M R_M \frac{L^n}{L^n + \Phi(L + K_1)^n} = I_M R_M F_{(AL_n)o} \qquad (1)$$

where $F_{(AL_n)o}$ is the fraction of receptor in the open-channel form, L is the molar concentration of the ligand ATP, n is the number of ligand-binding sites [$n = 3$ in the case of ATP binding to the $P2X_2$ receptor according to Ding and Sachs (*12*)], and K_1 is the dissociation constant for dissociation of the agonist ATP from the purinergic receptor. The channel opening equilibrium constant (Φ^{-1}) (*47*) is the ratio of channel opening (k_{op}) and channel closing (k_{cl}) rate constants; thus, $\Phi^{-1} = k_{op}/k_{cl}$. I_M is the current due to 1 mol of open receptor channels; R_M represents the number of moles of receptor in the cell membrane controlling channel opening, and $I_M R_M$ corresponds to the whole-cell current that would be observed if all the receptor channels opened in the presence of a saturating concentration of ligand (*49*).

A least-squares regression to the logistic equation was used to evaluate the constants (Prism, GraphPad Software, San Diego, CA). EC_{50} is the effective concentration of agonist that gives half-maximal amplitude, and n_H is the Hill coefficient. Antagonist concentration−response curves were fitted in the same manner to determine IC_{50} (inhibitory concentration resulting in 50% of maximal response) values. The inhibition constant (K_i) describes the affinity of the inhibitor for the receptor, and was estimated using the relationship $K_i = IC_{50}/(1 + L/EC_{50})$, assuming that inhibitor and ligand bind to the same site on the receptor (*50*).

Throughout the text, data are expressed as the mean ± the standard error of the mean. The data were considered statistically different when $p < 0.05$, using the unpaired Student's *t* test.

According to Breitinger et al. (*51*), Ramakrishnan and Hess (*52*), and Walstrom and Hess (*49*), the following equations were used to analyze the experiments:

Dose−Response Curve in the Presence of an Agonist. The plot of agonist concentration response can be linearized (*49*) and allows evaluation of Φ and K_1:

$$\left(\frac{A_{max}}{A} - 1\right)^{1/3} = \Phi^{1/3} + \Phi^{1/3}\frac{K_1}{L} \qquad (2)$$

Dose−Response Curve in the Presence of a Competitive Inhibitor.

$$A = \frac{A_{max}}{\left[\frac{K_1}{L}\left(1 + \frac{X}{K_i}\right) + 1\right]^3 (\Phi + 1)} \qquad (3)$$

where X is the concentration of inhibitor, K_i is the inhibition constant, and all the other constants have been described before. When the inhibitor concentration X is varied and the ligand concentration L remains constant, eq 3 can be linearized to study the dependence of obtained whole-cell current on inhibitor concentration:

$$\left(\frac{A_{max}}{A} - 1\right)^{1/3} = \Phi^{1/3}\left(1 + \frac{K_1}{L}\right) + \frac{XK_1}{K_i L}\Phi^{1/3} \qquad (4)$$

Noncompetitive Inhibition (53).

$$\left(\frac{A_{max}}{A} - 1\right)^{1/3} = \left(\Phi^{1/3} + \frac{K_1}{L}\Phi^{1/3}\right)Z \qquad (5)$$

$Z = (X/K_X + 1)^{1/3}$ when a noncompetitive inhibitor binds only to the closed-channel form of the receptor.

General Noncompetitive Inhibition.

$$\frac{A}{A_{i(X)}} = 1 + \frac{X}{K_X} \qquad (6)$$

where X represents the concentration of the inhibitor, A is the current amplitude in the presence of the agonist, and $A_{i(X)}$ is the current amplitude in the presence of the agonist and inhibitor X. This equation allows the determination of the dissociation constant of a noncompetitive inhibitor (K_X) from the receptor.

Competitive Inhibition.

$$\frac{A}{A_{i(X)}} = 1 + \frac{X}{K_i}\left[(3F_A + F_{AL}) + F_A\frac{X}{K_i}\right] \qquad (7)$$

F_A and F_{AL} are the fractions of unbound receptors and receptor species bound to one inhibitor molecule at equilibrium, respectively; for more details, see ref *51*. The equation for competitive inhibitors is reduced to that of noncompetitive inhibitors when the terms $F_A(X/K_i) \ll (3F_A + F_{AL})$ in the above-described equation, being the case at low inhibitor concentrations.

RESULTS

In this work, we have compared the inhibition mechanisms of the rat recombinant $P2X_2$ receptor by two purinergic receptor antagonists, TNP-ATP and suramin. As shown in Figure 1, TNP-ATP is an ATP analogue with a trinitrophenyl group added to the ribose moiety. The structural similarity of TNP-ATP and ATP suggests that both molecules may interact with the same binding site on P2X receptors. In the case of suramin, the same suggestion is not plausible.

We have used 1321N1 human glioma cells stably transfected with $P2X_2$ receptors as a model for studying $P2X_2$ receptor inhibition, since these cells do not express any endogenous functional purinergic receptors (*39*, *40*). We have verified the presence of $P2X_2$ receptors on the mRNA transcription and protein expression level. $P2X_2$ receptor gene expression was detected by RT-PCR. The amplified cDNA

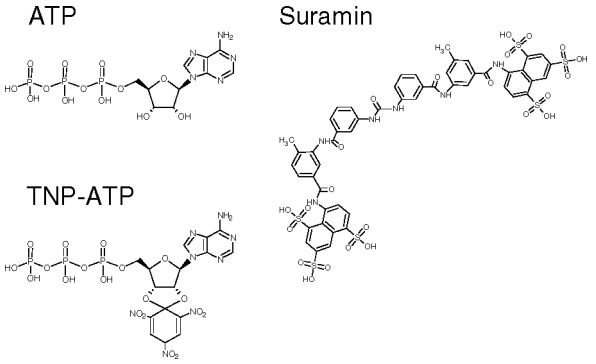

FIGURE 1: Chemical structures of the purinergic receptor agonist ATP and the antagonists TNP-ATP and suramin.

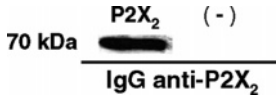

FIGURE 2: Detection of the $P2X_2$ receptor protein. Western blot analysis of plasma membrane protein extracts from stably transfected 1321N1 glial cells with recombinant rat $P2X_2$ receptors (left lane) or with the expression vector only as a control (right line) was carried out as described in Materials and Methods. The reaction was developed using the ECL chemiluminescence reaction (Pierce) followed by exposure to Kodak X-Omat film.

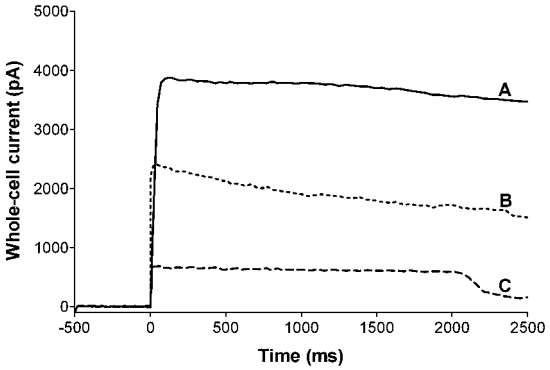

FIGURE 3: Cell-flow investigations of the effects of ATP, suramin, and TNP-ATP on rat $P2X_2$ receptors of 1321N1 glial cells. All measurements were carried out at pH 7.4 and 25 °C, with a fixed membrane voltage of −60 mV, using a rapid chemical kinetic technique and a flow rate of the ATP solution of 1 cm/s for the rapid equilibration of the cell surface receptor with the ligand (*41*, *42*). (A) Whole-cell current response of the receptors to 100 μM ATP. The observed whole-cell current (solid line) is a measure of the number of receptors in the open-channel form in the cell membrane and reached a maximum value in ~80 ms. The falling phase of the current, indicative of receptor desensitization, exhibits only one process. The rate coefficient for receptor desensitization (α) was 0.45 ± 0.1 s^{-1}. (B) Inhibition of the whole-cell current induced by 100 μM ATP in the presence of 20 μM suramin or (C) 50 μM TNP-ATP.

was confirmed to be identical to rat $P2X_2$ receptor cDNA as determined by DNA sequencing of the PCR product (GenBank accession number NM_053656) (data not shown). Western blot analysis revealed the presence of only one isoforms with a molecular mass of 70 kDa and no splice variants of the $P2X_2$ receptor (Figure 2).

Figure 3 shows a representative whole-cell current measurement performed in the presence of 100 μM ATP (A, solid line), 100 μM ATP with 20 μM suramin (B, dotted line), and 100 μM ATP with 50 μM TNP-ATP (C, dashed line), using the cell-flow technique (*41*, *42*). The current obtained with 100 μM ATP reached a maximum value within 80 ms, showing rapid receptor activation. In all experiments with more than 30 different cells at ATP concentrations ranging from 1 to 1000 μM, only one of these cells exhibited a significant desensitization rate. The slope was equal to -0.116 ± 0.006, and the rate coefficient for receptor desensitization (α) was 0.45 ± 0.1 s^{-1}, reflecting slow desensitization of receptors in the presence of the agonist. Co-application of TNP-ATP resulted in a reduction of the whole-cell current obtained in the presence of ATP, but did not interfere with the receptor desensitization as the rate coefficient for desensitization did not change ($\alpha = 0.40 \pm 0.06$ s^{-1}). Suramin application affected the amplitude of the whole-cell current, as well as the desensitization rate. The slope of current decay in the presence of suramin was -0.036 ± 0.002, and the rate coefficient that was obtained was 0.70 ± 0.17 s^{-1}.

Currents induced by ATP concentrations between 1 and 1000 μM ranged from 10 to 4971 pA (Figure 4A). The values of the constants accounting for the observed current due to channel opening were evaluated using a nonlinear fit of these data to eq 1. EC_{50} for receptor activation by ATP was determined to be 42 ± 2 μM ($R^2 = 0.98$), and the Hill slope was 2.11 ± 0.04 (solid line; $R^2 = 0.98$), suggesting the presence of three ATP binding sites for channel opening (*12*). A simulation with a Hill slope of <2 was created to investigate the possibility of binding of two ATP prior to channel opening (dotted line). In this situation, we observed a correlation index equal to 0.82 and a statistically different data fit ($p = 0{,}0438$), supporting the necessity of three ATP molecules for channel opening. The dissociation constant for binding of ATP to the receptor (K_1) was calculated as 38 ± 2 μM according to eq 2. The channel opening equilibrium constant (Φ^{-1}) as a measure of receptor activation in the presence of the agonist was 0.110 ± 0.012, following linearization of the dose-dependence curve of ATP (eq 2).

An ATP concentration of 100 μM which represents a condition where receptors are mainly in the open-channel form was used to determine inhibition constants for suramin and TNP-ATP. The data were replotted using linear regression for comparison of results obtained in the presence of TNP-ATP or suramin.

Inhibition of the $P2X_2$ Receptor by TNP-ATP. As expected, TNP-ATP by itself did not activate $P2X_2$ receptors in 1321N1 glioma cells (data not shown). However, TNP-ATP inhibited ATP-mediated whole-cell currents when co-applied with the neurotransmitter. The IC_{50} value of $P2X_2$ receptor inhibition by TNP-ATP was 9.4 ± 0.9 μM ($R^2 = 0.97$) with a Hill slope of -0.76 ± 0.70 (Figure 4B).

To determine whether TNP-ATP inhibits the $P2X_2$ receptor by competing with ATP for the ligand-binding site or by an independent noncompetitive mechanism, whole-cell currents obtained in the presence of 100 μM ATP and increasing concentrations of TNP-ATP (from 10 to 300 μM) were plotted as a function of antagonist concentration (Figure 5A). The channel opening equilibrium constant in the presence of TNP-ATP (Φ^{-1}) decreased from 0.110 ± 0.012 to 0.002 ± 0.001, indicating that the equilibrium between channel opening and closing was shifted to the closed channel form. When a single, identical binding site for both ATP and TNP-ATP was proposed, according to the method of Cheng and Prusoff (*50*), the dissociation constant for receptor inhibition by TNP-ATP (K_i) was calculated to be 3 ± 1 μM.

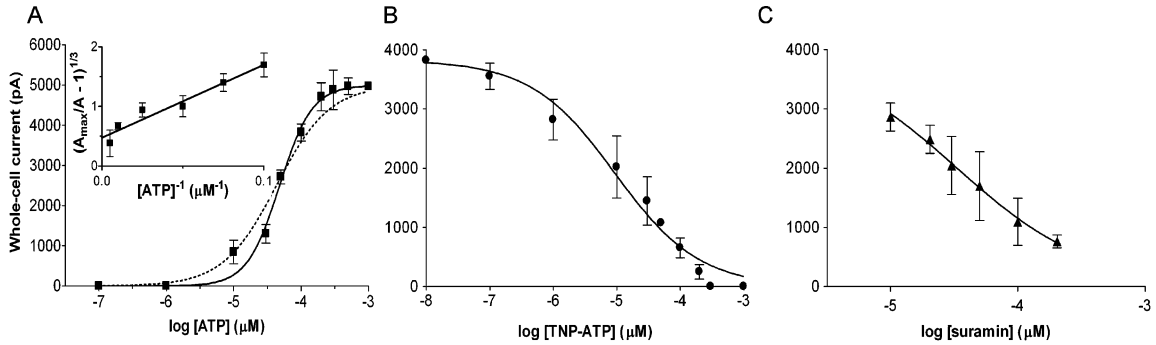

FIGURE 4: Dependence of obtained whole-cell currents on the concentrations of the agonist ATP and antagonists suramin and TNP-ATP. All measurements were carried out at pH 7.4 and 25 °C, with a fixed membrane voltage of −60 mV. (A) Dependence of current amplitudes on the concentration of ATP (■) obtained in cell-flow experiments. Each data point represents the mean value of 3−19 data points obtained from 49 cells. The currents of each cell with increasing concentrations of ATP were normalized to those obtained in the presence of 100 μM ATP. The current obtained in different cells in the presence of ATP ranged from 10 to 4971 pA. The Hill slope was 2.11 ± 0.04 (solid line). The EC_{50} value was determined to be 42 ± 2 μM ($R^2 = 0.98$). The dotted line is a simulation of two binding sites for channel opening (Hill slope was set to 1.8; $R^2 = 0.82$). The inset shows a linear curve fit of the same plot (eq 2). The linear fit of the data gave an intercept of 0.480 ± 0.002, resulting in the value for the channel opening equilibrium constant (Φ^{-1}) of 0.110 ± 0.012 and the dissociation constant for ATP−receptor binding (K_1) of 38 ± 2 μM. (B) Dependence of the current amplitudes obtained by 100 μM ATP on the concentration of TNP-ATP (●). Each data point represents the mean value of 5−14 data points obtained from 58 cells. Currents were normalized to those obtained with 100 μM ATP. Currents ranged from 0 to 3800 pA. The Hill slope was −0.76 ± 0.70. The IC_{50} value was 9.4 ± 0.9 μM ($R^2 = 0.97$). (C) Dependence of the current amplitudes obtained with 100 μM ATP on the concentration of suramin (▲). The presented data corresponding to each concentration of ATP are mean values from 3−10 measurements from a total of 35 cells. Currents were normalized to those obtained with 100 μM ATP alone. Currents ranged from 764 to 2680 pA. The Hill slope was−0.82 ± 0.04. The IC_{50} for inhibition by suramin was 34 ± 2 μM ($R^2 = 0.98$).

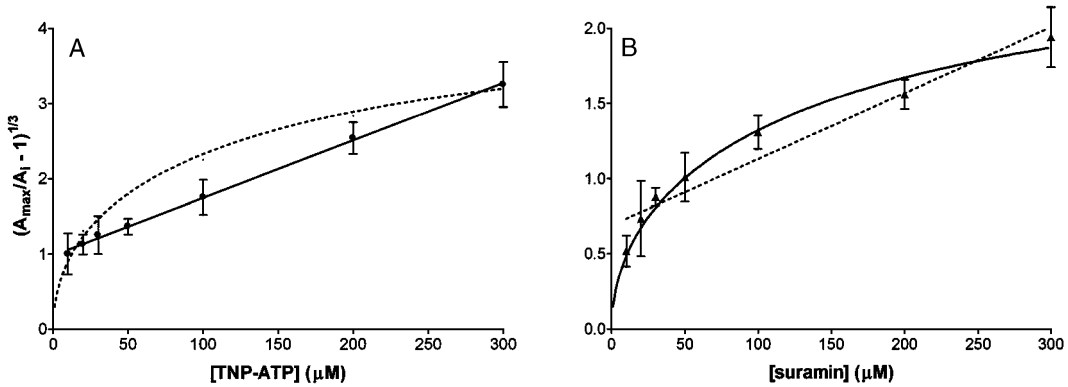

FIGURE 5: Inhibition of rat recombinant $P2X_2$ receptors by TNP-ATP and suramin. Experimental conditions were as described in the legends of Figures 3 and 4. Each data point includes three to six measurements each from a total of 38 cells at various TNP-ATP or suramin concentrations. (A) Inhibition of $P2X_2$ receptors by TNP-ATP (●) at a constant ATP concentration of 100 μM. Curve fitting was carried out according to eq 4 by simulation of linear (solid line, in the case of a competitive inhibitor) and nonlinear (dotted line, for a noncompetitive inhibitor) fits. The linear fit applied best for the data ($R^2 = 0.97$ and a slope of 0.0165 ± 0.0003 μM^{-1}) indicating a competitive mechanism. The channel opening equilibrium constant (Φ^{-1}) was equal to 0.002 ± 0.001, as calculated from the intercept. The constant for receptor inhibition by TNP-ATP (K_i) was calculated to be 3 ± 1 μM (*50*). (B) Inhibition of the $P2X_2$ receptors by suramin (▲) at a constant ATP concentration of 100 μM. For a noncompetitive inhibitor, a plot of $(A_{max}/A_i - 1)^{1/3}$ vs inhibitor concentration is expected to be nonlinear and to show a cube root dependence on inhibitor concentration, according to eq 5. The nonlinear fit (solid line) shows a correlation index of 0.97, indicating a nonlinear inhibition mechanism for the $P2X_2$ receptor by suramin. The dotted line provides a simulation of linear curve fitting.

The dose−response curve for ATP acting upon P2X receptors is shifted to higher concentrations of agonist in the presence of a competitive antagonist, and subsequently, EC_{50} values for ATP-induced receptor activation increase without a change in the maximum current (A_{max}). However, a noncompetitive inhibitor that binds preferentially to the closed-channel form can also account for these observations (*51*). Therefore, it is necessary to differentiate between a competitive inhibitor and a noncompetitive inhibitor that binds mainly to the closed-channel form and prevents receptor activation. Equation 4 predicts that the plot of $(A_{max}/A_i - 1)^{1/3}$ versus the concentration of a competitive inhibitor will be linear, whereas the curve fit for a noncompetitive inhibitor will be nonlinear. In the case of noncompetitive inhibition, $(A_{max}/A_i - 1)^{1/3}$ is proportional to the cube root of inhibitor concentration multiplied by a constant (eq 5).

The comparison of a nonlinear and a linear regression for curve fitting of TNP-ATP inhibition of the $P2X_2$ receptor activity, as shown in Figure 5A, indicates that a linear relationship fits the data better, consequently confirming a competitive inhibition mechanism. The data fitted by linear regression have a slope equal to 0.0165 ± 0.0004 μM^{-1} ($R^2 = 0.99$). In contrast, a plot for a noncompetitive inhibitor is expected to be a nonlinear curve fit, and this curve is simulated (dotted line) in Figure 5A.

The ratio of the current amplitudes obtained in cell-flow experiments in the absence, A, and presence, $A_{i(X)}$, of inhibitor (eq 7) can provide additional information about the inhibition

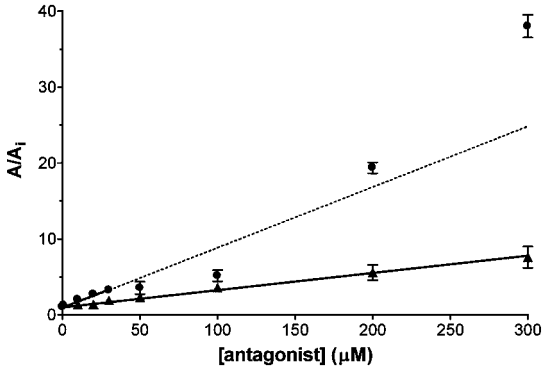

FIGURE 6: Inhibition of the $P2X_2$ receptors by TNP-ATP and suramin. Experimental conditions were as described in the legends of Figures 3 and 4. Inhibition of $P2X_2$ receptors by various concentrations of TNP-ATP (●) or suramin (▲) was studied at a constant ATP concentration of 100 μM. Three to six measurements were performed for each TNP-ATP or suramin concentration. A total of 38 cells were used for these measurements. The data were plotted according to eq 6 or 7 using an A_{max} of 3824 pA. (●) Inhibition by TNP-ATP. The slope of the fitted line was 0.076 ± 0.006 μM^{-1}, and the intercept was 1.13. The apparent inhibition constant (K_i) was 3.7 ± 0.2 μM (eq 7). Note the deviation from linearity at higher concentrations of the inhibitor (dotted line). (▲) Inhibition by suramin. The linear regression of the obtained data gave a slope of 0.023 ± 0.001 μM^{-1} and an intercept of 1.02 over the whole range of suramin concentrations. The apparent inhibition constant (K_x) was 38 ± 1 μM (eq 6). Note that the linear relation is still valid at higher inhibitor concentrations.

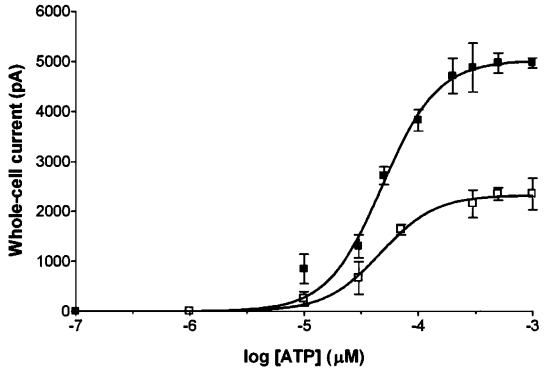

FIGURE 7: Dependence of the obtained whole-cell current on the concentration of agonist ATP in the absence (■) or presence (□) of 100 μM suramin. All measurements were carried out at pH 7.4 and 25 °C, with a fixed membrane voltage of −60 mV. The dependence of the obtained current amplitude on the concentration of ATP (■), as already demonstrated in Figure 4A, was determined by cell-flow experiments. The current obtained in the presence of 100 μM suramin (□) with three to nine measurements was determined at each concentration of ATP for a total of nine points from 22 cells. The obtained current ranged from 700 to 2348 pA. The Hill slope was 2.2 ± 0.3, and the EC_{50} was equal to 44.5 ± 1.4 μM (R^2 = 0.97).

mechanism. A linear relationship exists between $A/A_{i(X)}$ and the noncompetitive inhibitor concentration over a wide concentration range. In the case of a competitive inhibitor, however, the plot of the ratio of $A/A_{i(X)}$ versus competitive inhibitor concentration is expected to be linear only at low inhibitor concentrations, when $F_A(X/K_X)$ is small compared to $3F_A + F_{AL}$ (see eq 7). F_A and F_{AL} represent the fractions of receptors in form A and AL (in this case, A represents the active, non-desensitized receptor and L the neurotransmitter), respectively. Figure 6 shows plots of $A/A_{i(X)}$ versus increasing TNP-ATP concentrations (●) at a constant ATP concentration of 100 μM according to eq 7. As expected for competitive inhibitors, a linear relationship between $A/A_{i(X)}$ and TNP-ATP concentration was obtained only at low inhibitor concentrations in the range of 0−30 μM TNP-ATP. The inhibition constant obtained at a low concentration of TNP-ATP calculated by using eq 7 was found to be 3.7 ± 0.2 μM.

A radioligand binding assay was employed to corroborate and determine whether TNP-ATP (from 0.01 to 100 μM) and [α-^{32}P]ATP (200 000 cpm, 130 pM) compete for the same binding sites on the receptor. As demonstrated in Figure 8, TNP-ATP displaced [α-^{32}P]ATP from the ATP-binding site, and potently inhibited the specific binding of [α-^{32}P]-ATP to $P2X_2$ receptors with an IC_{50} equal to 2.7 ± 0.1 μM. This value is in agreement with that obtained from whole-cell current recording (Figures 5 and 6), confirming the competitive inhibition mechanism of $P2X_2$ receptors by TNP-ATP in living 1321N1 cells.

Inhibition of the $P2X_2$ Receptor by Suramin. Suramin alone did not activate $P2X_2$ receptors (data not shown). As expected, suramin inhibited ATP-induced whole-cell currents when co-applied with the neurotransmitter (Figure 3). The IC_{50} for inhibition of the $P2X_2$ receptor by suramin was 34 ± 2 μM (R^2 = 0.98) with a Hill slope of −0.82 ± 0.04 (Figure 4C). Preincubation of cells with 100 μM suramin for 10 min, a sufficient time for saturation of $P2X_2$ receptors with the inhibitor (*54*), increased the inhibition factor compared to that for the co-application of the same suramin concentration with ATP (data not shown). Inhibition of $P2X_2$ receptor activity in different tissues by suramin has previously been observed. Whether this inhibition is competitive or noncompetitive with ATP binding to the ligand site of the receptor is not yet well understood.

The results shown in Figure 5B indicate that suramin is a noncompetitive inhibitor of stably transfected 1321N1 glial cells expressing recombinant rat $P2X_2$ receptors in the concentration range from 10 to 300 μM. In the case of noncompetitive inhibition, the plot of $(A_{max}/A_i - 1)^{1/3}$ versus increasing antagonist concentration fits best to a nonlinear model, as $(A_{max}/A_i - 1)^{1/3}$ is proportional to the cube root of the inhibitor concentration (eq 5). Figure 5B shows that curve fitting of this plot is not linear (R^2 = 0.97), suggesting a noncompetitive inhibition mechanism in which suramin binds preferentially to the closed-channel form. In Figure 5B, the dotted line is a simulation of curve fitting by linear regression.

The following evidence further supports a noncompetitive inhibition mechanism for suramin. In contrast to the $A/A_{i(X)}$ inhibition ratio versus antagonist concentration plots with the inhibitor TNP-ATP, which is linear only at low concentrations, the analysis of the $A/A_{i(X)}$ inhibition ratio versus suramin concentration shows a linearity over the whole concentration range of suramin (from 1 to 300 μM) used in the experiment (Figure 6), indicating again a noncompetitive inhibition mechanism for suramin as predicted by eq 6. This equation allows the determination of the apparent dissociation constant (K_x) of the noncompetitive inhibitor binding to the receptor prior to desensitization (K_x = 38 ± 1 μM). The apparent channel opening equilibrium constant in the presence of suramin $\Phi^{-1\prime}$ is decreased (0.003 ± 0.002) compared to Φ^{-1} in the presence of ATP alone. Thus, in accordance

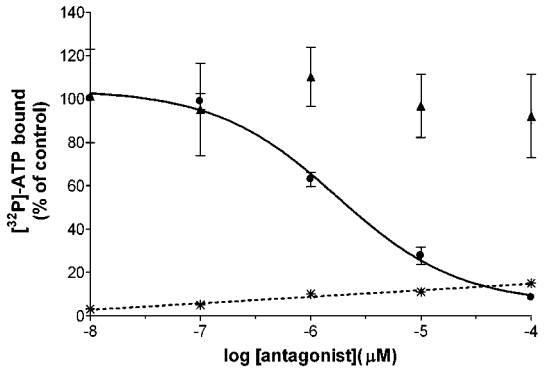

FIGURE 8: Displacement of [^{32}P]ATP from recombinant rat $P2X_2$ receptors expressed in 1321N1 cells using suramin (▲) and TNP-ATP (●) as competitors. The dotted line (*) represents the nonspecific binding of [α-^{32}P]ATP to 1321N1 cells expressing rat $P2X_2$ receptors in the presence of 100 μM unlabeled ATP. Experimental conditions are detailed in Materials and Methods. All measurements were carried out in triplicate. Note the displacement of [α-^{32}P]ATP in the presence of TNP-ATP with IC_{50} equal to 2.7 ± 0.1 μM and no interference of suramin with [α-^{32}P]ATP receptor binding.

with other published studies (*16*, *55*, *56*), suramin is a less effective inhibitor than TNP-ATP.

To provide further proof for the model of noncompetitive inhibition of the $P2X_2$ receptor by suramin, a classical experiment was performed by measuring ATP activation curves of receptor activity in the absence of suramin (■) and at a fixed suramin concentration (□, 100 μM) (Figure 7). The agonist-induced whole-cell current was inhibited by a factor of approximately 2 at various ATP concentrations. Concentration−response analysis revealed that 100 μM suramin attenuated the response to ATP, but did not alter the EC_{50} for ATP-receptor activation. In presence of suramin, the obtained EC_{50} for ATP activation was 44.5 ± 1.4 μM (Hill slope of 2.2 ± 0.3), compared to 42 ± 2 μM (Hill slope of 2.11 ± 0.04) in the presence of ATP alone. These data indicate and support a noncompetitive effect of suramin on the ATP action site.

Displacement of [α-^{32}P]ATP from recombinant rat $P2X_2$ receptors expressed in 1321N1 cells using suramin (▲) as a competitor in radioligand binding assays provided further evidence that ATP and suramin do not compete for the same binding site (Figure 8). Co-incubation of various concentrations of suramin (from 0.01 to 100 μM) and [α-^{32}P]ATP did not interfere with [α-^{32}P]ATP receptor binding. This result is in agreement with that obtained from whole-cell recording measurements shown in Figures 5−7, confirming the noncompetitive mechanism of inhibition of $P2X_2$ by suramin in living 1321N1 cells.

According to our results (Figures 5−8), the previously published explanation for an inhibition mechanism of the $P2X_2$ receptor by suramin (*24*) is not plausible. Our data support a competitive inhibition mechanism for TNP-ATP and a noncompetitive inhibition mechanism for suramin.

DISCUSSION

A rapid chemical kinetic technique with a 10 ms time resolution was used to investigate the mechanism of ATP activation and suramin and TNP-ATP inhibition of the rat $P2X_2$ receptor expressed in stably transfected 1321N1 glioma cells. The technique consists of rapidly exchanging ligand solutions on the cell surface (*42*) in combination with the whole-cell current recording technique (*43*) to measure the current due to channel openings of purinergic receptors that occurs while the cell surface equilibrates with ATP in the absence or presence of inhibitors.

Rat $P2X_2$ receptors exhibit a slow desensitization process, as determined by the rate coefficient of desensitization (α), and the decay of the response contains one desensitizing component which could be described as a single-exponential process not significantly changing at different ATP concentrations. Thus, the kinetics of channel activation and the pharmacological properties of the $P2X_2$ receptor in 1321N1 glial cells are consistent with previously reported observations (*16*), establishing a representative assay system for pharmacological characterization of this receptor.

We have determined a Hill coefficient of 2.11 for ATP activation of the $P2X_2$ receptor. These results are similar to those obtained by Brake et al. (*5*) and Ding and Sachs (*12*) who measured Hill coefficients of 2.0 and 2.3, respectively. Although the Hill coefficient in some published studies (*57*, *58*) suggests two binding sites for ATP, a model indicating binding of three ligand molecules prior to channel opening based on results obtained by single-channel recording is widely accepted (*12*, *20*). This work corroborates the model based on the binding of three ATP molecules for channel activation. The discrepancy of an overly small Hill coefficient and a three-binding site model can be minimized by connecting an ATP-independent closed state to the open states (*12*).

We have studied the mechanisms of inhibition of the rat $P2X_2$ receptor by TNP-ATP, a structural analogue of ATP, and suramin, the most relevant antagonist of purinergic receptor, which is not structurally similar with ATP. Hypotheses published on the inhibition of P2X receptors by TNP-ATP include competitive as well as noncompetitive mechanisms. For instance, Virginio et al. (*38*) described a noncompetitive mechanism for inhibition of P2X receptors. However, a competitive inhibition mechanism of TNP-ATP on heteromeric rat $P2X_{2/3}$ receptors has been described by Burgard et al. (*37*). The latter observations are supported by our experimental data, as follows.

First, the inhibition of $P2X_2$ receptor activity could be overcome by increasing agonist concentrations.

Second, data obtained from whole-cell current recordings performed at a constant concentration of ATP and at various concentrations of TNP-ATP, based on eq 4, obeyed a typical competitive linear curve fitting when $(A_{max}/A_i - 1)^{1/3}$ was plotted versus inhibitor concentration (Figure 5B), and allowed to determine the channel opening equilibrium (Φ^{-1}) and inhibition constants (K_i) of the receptor in the presence of TNP-ATP. This method had already been used to differentiate between competitive and noncompetitive inhibition of the serotonin 5-HT_3 receptor by nicotine, cocaine, and fluoxetine (*51*).

Third, the ratio of the current amplitudes obtained in cell-flow experiments in the absence and presence of inhibitor (eq 7) gave additional support for a competitive mechanism of inhibition by TNP-ATP. According to Breitinger et al. (*51*) and Ramakrishnan and Hess (*52*), a linear relationship exists between $A/A_{i(X)}$ and inhibitor concentration over a wide concentration range in the case of a noncompetitive inhibitor such as suramin (0−300 μM). In the case of TNP-ATP,

linearity between $A/A_{i(X)}$ and inhibitor concentration exists only for a narrow concentration range (0−30 μM), indicating a competitive mechanism for $P2X_2$ receptor inhibition. For instance, a proof for the inhibition mechanism of the $GABA_A$ receptor was obtained by using eq 7 (*52*).

Finally, a competitive mechanism of inhibition of the $P2X_2$ receptor by TNP-ATP was supported by results from radioligand−receptor binding assays, where TNP-ATP displaced [α-^{32}P]ATP from its binding site on $P2X_2$ receptors in 1321N1 cells. The dissociation constant determined by binding assays is in agreement with those obtained from whole-cell measurements, indicating that TNP-ATP, in fact, is a competitive antagonist of nondesensitizing $P2X_2$ receptors.

Several published studies suggested that suramin is a competitive antagonist of P2X receptors (*24*−*27*). However, our data have provided clear evidence that suramin has the characteristics of a noncompetitive inhibitor for the $P2X_2$ receptor and does not compete with ATP for the ligand-binding site on the receptor. Plotting $A/A_{i(X)}$ versus inhibitor concentration allows us to determine the apparent dissociation constant (K_x) of a noncompetitive antagonist. As expected for a noncompetitive inhibitor, a linear relationship existed over a 200-fold range of suramin concentrations.

Nonlinear curve fitting of $(A_{max}/A_i - 1)^{1/3}$ versus inhibitor concentration indicates that suramin is a noncompetitive inhibitor which binds to a closed-channel form of the receptor. Moreover, the dependence of the obtained whole-cell current on the concentration of the agonist ATP is identical in the absence or presence of a constant suramin concentration. As the EC_{50} was not changed in these experiments, our data indicate a classical noncompetitive inhibition mechanism for suramin.

The results of experiments measuring the level of [α-^{32}P]-ATP−receptor binding in the presence and absence of suramin showed that suramin did not interfere with [α-^{32}P]-ATP−receptor binding when co-applied with the radioligand to the cells. Discrepancies between receptor binding properties of suramin in different tissues have been reported (*21*, *24*, *25*). However, we note that in the equilibrium binding experiments, in which displacement of a radioligand is used to determine the affinity of an inhibitor like suramin to the receptor, it is not known whether the measurements reflect the binding to the receptor before or after desensitization, or even binding to sites other than on the ATP receptor. These ambiguities are avoided by analyzing binding studies in association with kinetic experiments where one measures the effect of the specific receptor ligand ATP and an inhibitor on the current resulting from the opening of ATP-activated transmembrane channels (*51*). In addition, we can ensure that the obtained current in the presence of ATP results only from $P2X_2$ receptor activation because 1321N1 cells do not express endogenous purinergic receptors (*39*, *40*), whereas ATP and suramin may bind to other proteins on the cell surface.

Claims that suramin is a competitive inhibitor of purinergic receptors go back to 1990 (*24*), when the $P2X_2$ receptor had not yet been isolated (*5*). Leff and co-workers described suramin as a slowly equilibrating, competitive antagonist of P2X receptors in isolated ear arteries from rabbit. Most of those studies indicating a competitive inhibition mechanism for suramin on P2X receptors were carried out using tissue preparations which express a variety of purinergic receptors (*24*−*26*). Bianchi and co-workers (*17*) employed calcium influx assays to study competitive properties of suramin as a competitive inhibitor. This methodology commonly has a low time resolution, mostly due to slow ligand exchange during the measurements. The maximal resolution of fluorescence-based calcium influx assays is in the scale of seconds, and these measurements are possibly affected by interference of calcium-reporting fluorophores. Fast kinetic whole-cell recording (cell-flow measurements) achieves a time resolution of 10 ms, reflecting the direct action of the ligand on the receptor. Wong and co-workers (*28*) have studied P2X receptor inhibition by suramin in rat hippocampal granule cells using single-channel recording, and have concluded that a competitive inhibition mechanism for suramin would not be consistent.

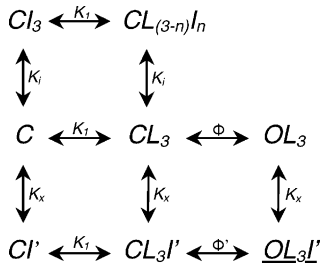

FIGURE 9: Proposed model for the inhibition mechanism of $P2X_2$ receptors, according to refs *12* and *51*. *C* represents the closed, active, non-desensitized receptor and *L* the neurotransmitter; the subscripts *3* and *n* ($0 \leq n \leq 3$) indicate the number of receptor-bound ligand molecules. *O* represents the open-channel form of the receptor. K_1 (38 ± 2 μM) is the dissociation constant for dissociation of the ligand (ATP) from the receptor site controlling channel opening, and Φ^{-1} was 0.110 ± 0.012. *I* represents the competitive inhibitor TNP-ATP, and K_i (3 ± 1 μM) is the dissociation constant for dissociation of TNP-ATP from the receptor. *I*′ represents the noncompetitive inhibitor suramin. It is assumed in the model that only a single apparent dissociation constant K_x exists for the noncompetitive inhibitor suramin (38 ± 1 μM) (for instance, *I*′ binds equally well to all channel forms). The channel opening equilibrium constant in the presence of suramin, Φ' (0.003 ± 0.002), is decreased, resulting in fewer channels in the open form (OL_3I').

Thus, our work is the first using a rapid chemical kinetic technique to compare kinetics and is the basis of understanding the inhibition mechanism of TNP-ATP and suramin on the $P2X_2$ receptor expressed in a uniform and silent background. Although purinergic receptors share an endogenous agonist in vivo, they may have different functions on the basis of tissue distribution, activation kinetics, structure, and isoforms of the receptor. Moreover, the investigation of the $P2X_2$ receptor in vivo is hindered by the identification of up to six different splice variants of the rat homologue (*59*).

Our data obtained from both radioligand binding and fast kinetic whole-recording studies strongly support a noncompetitive mechanism of inhibition of the rat recombinant $P2X_2$ receptor by suramin and confirm the competitive inhibition by TNP-ATP. Thus, we suggest the following inhibition mechanism (Figure 9). TNP-ATP displaces ATP from its ligand-binding sites on the receptor, thereby preventing channel opening. Suramin binds to an allosteric, regulatory site on the receptor, different from the ligand-binding site. The presence of suramin induces a conformational change in the closed-channel form of the receptor protein, subse-

quently inhibiting channel opening in the presence of the ligand ATP. The existence of more than one binding site for suramin on the $P2X_2$ receptor cannot be ruled out.

These observations, obtained by a fast kinetic approach, permit the determination of constants for a chemical mechanism by which these receptors are activated and inhibited as a function of time and over a wide range of neurotransmitter and inhibitor concentrations, thus contributing to the knowledge of the signaling process in the nervous system and the development of therapies for disorders associated with purinergic receptor dysfunction (*60*, *61*).

ACKNOWLEDGMENT

The Center for Applied Toxicology, Butantan Institute, São Paulo, Brazil, is acknowledged for performing DNA sequencing.

REFERENCES

1. Neary, J. T., Rathbone, M. P., Cattabeni, F., Abbracchio, M. P., and Burnstock, G. (1996) Trophic actions of extracellular nucleotides and nucleosides on glial and neuronal cells, *Trends Neurosci. 19*, 13−18.
2. Abbracchio, M. P., and Burnstock, G. (1998) Purinergic signalling: Pathophysiological roles, *Jpn. J. Pharmacol. 78*, 113−145.
3. Burnstock, G. (1996) Purinoceptors: Ontogeny and phylogeny, *Drug Dev. Res. 39*, 204−242.
4. Ralevic, V., and Burnstock, G. (1998) Receptors for purines and pyrimidines, *Pharmacol. Rev. 50*, 413−492.
5. Brake, A. J., Wagenbach, M. J., and Julius, D. (1994) New structural motif for ligand-gated ion channel defined by an ionotropic ATP receptor, *Nature 371*, 519−523.
6. Nicke, A., Baumert, H. G., Rettinger, J., Eichele, A., Lambrecht, G., Mutschler, E., and Schmalzing, G. (1998) P2X1 and P2X3 receptors form stable trimers: A novel structural motif of ligand-gated ion channel, *EMBO J. 17*, 3016−3028.
7. Jiang, L. H., Kim, M., Spelta, V., Bo, X., Surprenant, A., and North R. A. (2003) Subunit arrangement in P2X receptors, *J. Neurosci. 26*, 8903−8910.
8. Barrera, N. P., Ormond, S. J., Henderson, R. M., Murrell-Lagnado, R. D., and Edwardson, J. M. (2005) Atomic force microscopy imaging demonstrates that P2X2 receptors are trimers but that P2X6 receptor subunits do not oligomerize, *J. Biol. Chem. 280*, 10759−10765.
9. Kim, M., Yoo, O. J., and Choe, S. (1997) Molecular assembly of the extracellular domain of $P2X_2$ an ATP-gated ion channel, *Biochem. Biophys. Res. Commun. 240*, 618−622.
10. Lewis, C., Neidhart, S., Holy, C., North, R. A., Buell, G., and Surprenant, A. (1995) Coexpression of P2X2 and P2X3 receptor subunits can account for ATP-gated currents in sensory neurons, *Nature 377*, 432−435.
11. Torres, G. E., Haines, W. R., Egan, T. M., and Voigt, M. M. (1998) Co-expression of P2X1 and P2X5 receptor subunits reveals a novel ATP-gated ion channel, *Mol. Pharmacol. 54*, 989−993.
12. Ding, S., and Sachs, F. (1999) Single channel properties of $P2X_2$ purinoceptors, *J. Gen. Physiol. 113*, 695−720.
13. Gonzalez, F. A., Weisman, G. A., Erb, L., Seye, C. I., Sun, G. Y., Velazquez, B., Hernandez-Perez, M., and Chorna, N. E. (2005) Mechanisms for inhibition of P2 receptor-mediated signaling pathways, *Mol. Neurobiol. 31*, 65−79.
14. Connolly, G. P. (1995) Differentiation by pyridoxal 5-phosphate, PPADS and IsoPPADS between responses mediated by UTP and those evoked by α,β-methylene-ATP on rat sympathetic ganglia, *Br. J. Pharmacol. 114*, 727−731.
15. Bultmann, R., Wittenburg, H., Pause, B., Kurz, G., Nickel, P., and Starke, K. (1996) P2-purinoceptor antagonists: III. Blockade of P2-purinoceptor subtypes and ectonucleotidases by compounds related to suramin, *Naunyn-Schmiedebergs Arch. Pharmacol. 354*, 498−504.
16. Khakh, B. S., Burnstock, G., Kennedy, C., King, B. F., North, R. A., Seguela, P., Voigt, M., and Humphrey, P. P. (2001) International union of pharmacology. XXIV. Current status of the nomenclature and properties of P2X receptors and their subunits, *Pharmacol. Rev. 53*, 107−118.
17. Bianchi, B. R., Lynch, K. J., Touma, E., Niforatos, W., Burgard, E. C., Alexander, K. M., Park, H. S., Yu, H., Metzger, R., Kowaluk, E. A., Jarvis, M. F., and van Biesen, T. (1999) Pharmacological characterization of recombinant human and rat P2X receptor subtypes, *Eur. J. Pharmacol. 376*, 127−138.
18. North, R. A., and Surprenant, A. (2000) Pharmacology of cloned P2X receptors, *Annu. Rev. Pharmacol. Toxicol. 40*, 563−580.
19. Dunn, P. M., and Blakeley, A. G. (1988) Suramin: A reversible P2-purinoceptor antagonist in the mouse vas deferens, *Br. J. Pharmacol. 93*, 243−245.
20. North, R. A. (2002) Molecular physiology of P2X receptors, *Physiol. Rev. 82*, 1013−1067.
21. Khakh, B. S., Michel, A., and Humphrey, P. P. (1994) Estimates of antagonist affinities at P2X purinoceptors in rat vas deferens, *Eur. J. Pharmacol. 263*, 301−309.
22. Surprenant, A. (1996) Functional properties of native and cloned P2X receptors, *Ciba Found. Symp. 198*, 208−219.
23. Blakeley, A. G., Dunn, P. M., and Petersen, S. A. (1988) A study of the actions of P1-purinoceptor agonists and antagonists in the mouse vas deferens in vitro, *Br. J. Pharmacol. 94*, 37−46
24. Leff, P., Wood, B. E., and O'Connor, S. E. (1990) Suramin is a slowly-equilibrating but competitive antagonist at P2x-receptors in the rabbit isolated ear artery, *Br. J. Pharmacol. 101*, 645−649.
25. Balcar, V. J., Li, Y., Killinger, S., and Bennett, M. R. (1995) Autoradiography of P2x ATP receptors in the rat brain, *Br. J. Pharmacol. 115*, 302−306.
26. Zhong, Y., Dunn, P. M., Xiang, Z., Bo, X., and Burnstock, G. (1998) Pharmacological and molecular characterization of P2X receptors in rat pelvic ganglion neurons, *Br. J. Pharmacol. 125*, 771−781.
27. Wildman, S. S., King, B. F., and Burnstock, G. (1998) Zn^{2+} modulation of ATP responses at recombinant $P2X_2$ receptors and its dependence on extracellular pH, *Br. J. Pharmacol. 123*, 1214−1220.
28. Wong, A. Y., Burnstock, G., and Gibb, A. J. (2000) Single channel properties of P2X ATP receptors in outside-out patches from rat hippocampal granule cells, *J. Physiol. 527*, 529−547.
29. Hiratsuka, T., and Uchida, K. (1973) Preparation and properties of 2′(or 3′)-O-(2,4,6-trinitrophenyl) adenosine 5′-triphosphate, an analog of adenosine triphosphate, *Biochim. Biophys. Acta 320*, 635−647.
30. Watanabe, T., and Inesi, G. (1982) The use of 2′,3′-O-(2,4,6-trinitrophenyl) adenosine 5′-triphosphate for studies of nucleotide interaction with sarcoplasmic reticulum vesicles, *J. Biol. Chem. 257*, 11510−11516.
31. Mockett, B. G., Housley, G. D., and Thorne, P. R. (1994) Fluorescence imaging of extracellular purinergic receptor sites and putative ecto-ATPase sites on isolated cochlear hair cells, *J. Neurosci. 14*, 6992−7007.
32. King, B. F., Wildman, S. S., Ziganshina, L. E., Pintor, J., and Burnstock, G. (1997) Effects of extracellular pH on agonism and antagonism at a recombinant P2X2 receptor, *Br. J. Pharmacol. 121*, 1445−1453.
33. Lewis, C. J., Surprenant, A., and Evans, R. J. (1998) 2′,3′-O-(2,4,6-Trinitrophenyl) adenosine 5′-triphosphate (TNP-ATP): A nanomolar affinity antagonist at rat mesenteric artery P2X receptor ion channels, *Br. J. Pharmacol. 124*, 1463−1466.
34. Thomas, S., Virginio, C., North, R. A., and Surprenant, A. (1998) The antagonist trinitrophenyl-ATP reveals co-existence of distinct P2X receptor channels in rat nodose neurons, *J. Physiol. 509*, 411−417.
35. Burgard, E. C., Niforatos, W., van Biesen, T., Lynch, K. J., Touma, E., Metzger, R. E., Kowaluk, E. A., and Jarvis, M. F. (1999) P2X receptor-mediated ionic currents in dorsal root ganglion neurons, *J. Neurophysiol. 82*, 1590−1598.
36. Grubb, B. D., and Evans, R. J. (1999) Characterization of cultured dorsal root ganglion neuron P2X receptors, *Eur. J. Neurosci. 11*, 149−154.
37. Burgard, E. C., Niforatos, W., van Biesen, T., Lynch, K. J., Kage, K. L., Touma, E., Kowaluk, E. A., and Jarvis, M. F. (2000) Competitive antagonism of recombinant P2X(2/3) receptors by 2′,3′-O-(2,4,6-trinitrophenyl) adenosine 5′-triphosphate (TNP-ATP), *Mol. Pharmacol. 58*, 1502−1510.
38. Virginio, C., Robertson, G., Surprenant, A., and North, R. A. (1998) Trinitrophenyl substituted nucleotides are potent antagonists selective for P2X1, P2X3, and heteromeric P2X2/3 receptors, *Mol. Pharmacol. 53*, 969−973.

39. Parr, E. C., Sullivan, D. M., Paradiso, A. M., Lazarowski, E. R., and Turner, J. T. (1994) Cloning and expression of a human P2U nucleotide receptor, a target for cystic fibrosis pharmacotherapy, *Med. Sci. 91*, 3275−3279.
40. Garrad, R. C., Otero, M. A., Erb, L., Theiss, P. M., Clarke, L. L., Gonzalez, F. A., Turner, J. T., and Weisman, G. A. (1998) Structural basis of agonist-induced desensitization and sequestration of the P2Y2 nucleotide receptor. Consequences of truncation of the C terminus, *J. Biol. Chem. 273*, 29437−29444.
41. Krishtal, O., and Pidoplichko, V. I. (1980) A receptor for protons in the nerve cell membrane, *Neuroscience 5*, 2324−2327.
42. Udgaonkar, J. B., and Hess, G. P. (1987) Chemical kinetic measurements of a mammalian acetylcholine receptor using a fast reaction technique, *Proc. Natl. Acad. Sci. U.S.A. 84*, 8758−8762.
43. Hamill, O. P., Marty, A., Neher, E., Sakmann, B., and Sigworth, F. J. (1981) Improved patch-clamp techniques for high-resolution current recording from cells and cell-free membrane patches, *Pfluegers Arch. 391*, 85−100.
44. Friel, D. D. (1988) An ATP-sensitive conductance in single smooth muscle cells from the rat vas deferens, *J. Physiol. 401*, 361−380.
45. Michel, A. D., Lundstrom, K., Buell, G. N., Surprenant, A., Valera, S., and Humphrey, P. P. (1996) The binding characteristics of a human bladder recombinant P2X purinoceptor, labelled with [^{3}H]-$\alpha\beta$-meATP, [^{35}S]-ATP γ-S or [^{33}P]-ATP, *Br. J. Pharmacol. 117*, 1254−1260.
46. Bradford, M. M. (1976) A rapid and sensitive method for the quantization of microgram quantities of protein utilizing the principle of protein-dye binding, *Anal. Biochem. 72*, 248−254.
47. Cash, D. J., and Hess, G. P. (1980) Molecular mechanism of acetylcholine receptor-controlled ion translocation across cell membranes, *Proc. Natl. Acad. Sci. U.S.A. 77*, 842−846.
48. Hess, G. P., Cash, D. J., and Aoshima, H. (1983) Acetylcholine receptor-controlled ion translocation: Chemical kinetic investigations of the mechanism, *Annu. Rev. Biophys. Bioeng. 12*, 443−473.
49. Walstrom, K. M., and Hess, G. P. (1994) Mechanism for the channel-opening reaction of strychnine-sensitive glycine receptors on cultured embryonic mouse spinal cord cells, *Biochemistry 33*, 7718−7730.
50. Cheng, Y., and Prusoff, W. H. (1973) Relationship between the inhibition constant (K_1) and the concentration of inhibitor which causes 50% inhibition (IC_{50}) of an enzymatic reaction, *Biochem. Pharmacol. 22*, 3099−3108.
51. Breitinger, H. G., Geetha, N., and Hess, G. P. (2001) Inhibition of the serotonin 5-HT3 receptor by nicotine, cocaine, and fluoxetine investigated by rapid chemical kinetic techniques, *Biochemistry 40*, 8419−8429.
52. Ramakrishnan, L., and Hess, G. P. (2005) Picrotoxin Inhibition Mechanism of a γ-Aminobutyric Acid(A) Receptor Investigated by a Laser-Pulse Photolysis Technique, *Biochemistry 44*, 8523−8532.
53. Shiono, S., Takeyasu, K., Udgaonkar, J. B., Delcour, A. H., Fujita, N., and Hess, G. P. (1984) Regulatory properties of acetylcholine receptor: Evidence for two different inhibitory sites, one for acetylcholine and the other for a noncompetitive inhibitor of receptor function (procaine), *Biochemistry 23*, 6889−6893.
54. Rettinger, J., Schmalzing, G., Damer, S., Muller, G., Nickel, P., and Lambrecht, G. (2000) The suramin analogue NF279 is a novel and potent antagonist selective for the P2X(1) receptor, *Neuropharmacology 39*, 2044−2053.
55. Honore, P., Mikusa, J., Bianchi, B., McDonald, H., Cartmell, J., Faltynek, C., and Jarvis, M. F. (2002) TNP-ATP, a potent P2X3 receptor antagonist, blocks acetic acid-induced abdominal constriction in mice: Comparison with reference analgesics, *Pain 96*, 99−105.
56. Fu, X. W., Nurse, C. A., and Cutz, E. (2004) Expression of functional purinergic receptors in pulmonary neuroepithelial bodies and their role in hypoxia chemotransmission, *Biol. Chem. 385*, 275−284.
57. Inoue, R., and Brading, A. F. (1990) The properties of the ATP-induced depolarization and current in single cells isolated from the guinea-pig urinary bladder, *Br. J. Pharmacol. 100*, 619−625.
58. Silberberg, S. D., Chang, T. H., and Swartz, K. J. (2005) Secondary structure and gating rearrangements of transmembrane segments in rat P2X4 receptor channels, *J. Gen. Physiol. 125*, 347−359.
59. Simon, J., Kidd, E. J., Smith, P. M., Chessell, I. P., Murrell-lagnado, R., Humphrey, P. P., and Barnard, E. A. (1997) Localization and functional expression of splice variants of the P2X2 receptor, *Mol. Pharmacol. 52*, 237−248.
60. Inoue, K., Koizumi, S., and Ueno, S. (1996) Implication of ATP receptors in brain functions, *Prog. Neurobiol. 50*, 483−492.
61. Franke, H., and Illes, P. (2005) Involvement of P2 receptors in the growth and survival of neurons in the CNS, *Pharmacol. Ther.* (in press).

BI051517W